

Modelling of Penny-Shaped Crack growth in Axisymmetric FGM with Residual Stresses

A.N. Galybin^{1,a}, L.I. Krenev^{2,b} and S.M. Aizikovich^{2,c}

¹ Institute of Physics of the Earth, RAS, Moscow, Russia

² Don State Technical University, 344000, Gagarina sq. 1, Rostov-on-Don, Russia

^a a.n.galybin@gmail.com, ^b lkrenev@yandex.ru, ^c saizikovich@gmail.com

Keywords: penny-shaped crack, FGM, residual stresses, semi-analytical methods.

Abstract. An axisymmetric static problem for a penny-shaped crack in heterogeneous isotropic elastic space is considered. It is assumed axisymmetric distributions of the Young modulus, Poisson's ratio and residual stresses coaxial with the crack axis. The elastic moduli vary in orthogonal direction to the crack plane in accordance with specific laws. The analysis is performed for the case of co-sinusoidal distributions of the residual stresses, for which we compute the mode I stress intensity factors for the crack during its quasistatic growth.

Introduction

The development of numerical methods for analysing crack propagation in Functionally Graded Materials (FGM) is an important problem of material sciences. In this study a 3D problem of elastostatics addressing the quasistatic growth of a penny-shaped crack in a heterogeneous isotropic FGM medium subjected to axisymmetric external and residual loads is considered. The method utilises the previously developed analytical approach reported in [1] that is applicable for axisymmetric problems in FGM. The aim of this study is to model the presence of residual stresses in FGM (that can be created during the process of manufacturing) and to investigate what is the influence of those on the fracture characteristics of the heterogeneous material possessing certain specific distributions of its elastic moduli. The residual stresses, in general, should be in static equilibrium, thus their 3D distribution cannot be selected arbitrary. Here we employ the method applied in [2] for modelling of the static trajectory of a curvilinear crack in elastic plate subjected (apart from external loads) to residual stress that manifest themselves as fluctuations of the total stress field. It has been suggested to take the residual stress into account by introducing random normal and shear loads of certain level on the crack surfaces. These can be introduced independently, which does not require the modelling of the total residual stress field at every point of the plate. In this study we accept that the level of the shear component of the residual stresses acting on the crack surfaces is negligible compare to the normal stresses. This assumption allows one to apply the technique based on dual integral equations developed in [3].

Crack in FGM half-space.

An isotropic heterogeneous elastic space with a disc-like crack is considered. It is assumed that the space obeys polar symmetry with respect to a cylindrical coordinate frame (r, φ, z) and the elastic moduli depend on the depth (i.e. vary along the z -axis). It is assumed that a crack develops in the direction orthogonal to the axis of symmetry $(0, \varphi, z)$. It is also assumed that the plane $z=0$ is the plane of symmetry of the stress/displacement fields and the mechanical properties of the material. This allows one to restrict the analysis of the stress state to the lower half-space Ω .

Let us assume that Poisson's coefficient, ν , is constant throughout the space, for simplicity $\nu=0.25$ and the Young modulus in the plane of symmetry varies in accordance with the following six laws of heterogeneity

$$E(z) = E^S \begin{cases} f_i(z), & -H \leq z \leq 0 \\ 1, & -\infty < z < -H \end{cases} \quad (1)$$

where E^S is the Young modulus at infinity and the functions $f_i(z)$ ($i=1,2\dots6$) are as follows (they are graphically shown in Fig. 1)

$$f_1(z) = 3.5, f_2(z) = \frac{1}{3.5}, f_3(z) = 3.5 + 2.5 \frac{z}{H}, f_4(z) = \frac{1}{3.5} - \frac{2.5}{3.5} \frac{z}{H}, f_5(z) = 1 + 2.5 \sin\left(\frac{\pi z}{H}\right), f_6(z) = 1 - \frac{2.5}{3.5} \sin\left(\frac{\pi z}{H}\right) \quad (2)$$

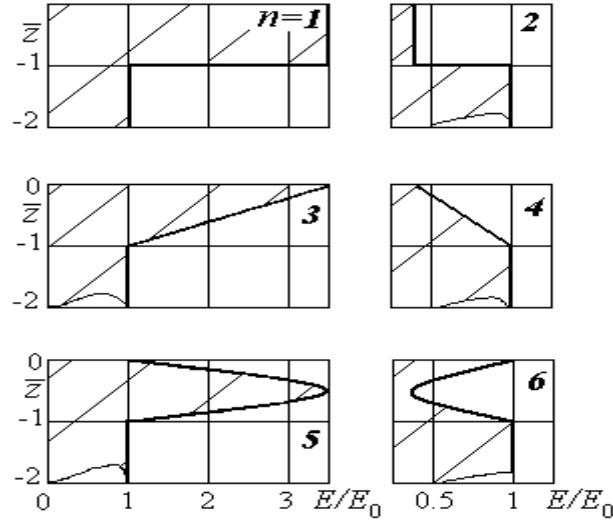


Fig. 1. Moduli distribution with depth

It is further assumed that the crack surfaces are loaded by uniformly distributed pressure of unit intensity combined with the co-sinusoidal distribution of normal residual stresses in the direction of the r -axis with the maximum intensity of about 10-20% of the uniform pressure.

The total load acting on the crack surfaces can be presented through the series of Bessel's functions (which is convenient for further calculations) in the form:

$$p^*(r) = p + \sum_{i=1}^{\infty} G_i J_1(\mu_i r); \quad \sum_{i=1}^{\infty} |C_i \lambda_i| \leq M_1(-1,1) < \infty \quad (3)$$

Here μ_k ($k=1,2,\dots$) are the positive roots of the following equation

$$\alpha J_1(r) + \beta r J_1'(r) = 0 \quad (4)$$

They are put in increasing order, $\alpha/\beta + 1 > 0$, α and β are given real numbers $M_1(-1,1)$ is a constant. The coefficients G_i are determined by the formula

$$G_i = 2 \left(1 + \frac{\alpha^2 - \beta^2}{\beta^2 \mu_i^2} \right)^{-1} J_1^2(\mu_i) \int_0^1 r p^*(r) J_1(\mu_i r) dr \quad (5)$$

Fig. 2 illustrates the profile of the loads applied to the crack surfaces. The solid curve marked by index 1 shows the load and the dotted line 2 corresponds to the approximation by Bessel's functions

(Eq.3-5). Further consideration is limited to the case when the radius of the crack varies from $0.25H$ to $4H$ (where H in the thickness of inhomogeneity, as specified by Eq 1-2).

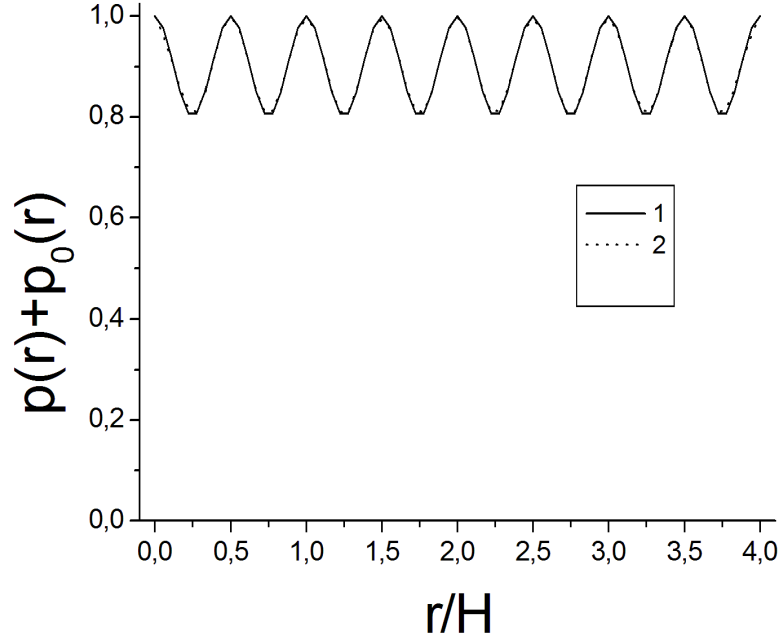


Fig. 2. Load (curve 1) and its approximation (curve 2) used in further calculations.

Based on the solution presented in [1] for the crack subjected to normal pressure, the crack opening displacements, $\delta(r)$, assumes the form

$$\delta(r) = \frac{2}{\pi} \left(-\frac{p}{\Delta(0)} \right) \left[L_N(\lambda \varepsilon) \int_r^1 \frac{\sin \varepsilon t dt}{\varepsilon \sqrt{t^2 - r^2}} + \sum_{k=1}^{\infty} L_N(\lambda \mu_k) G_k \int_r^1 \frac{\sin \mu_k t dt}{\sqrt{t^2 - r^2}} + \sum_{i=1}^N C_i \tilde{b}_i \int_r^1 \frac{\text{sh } \tilde{b}_i t dt}{\sqrt{t^2 - r^2}} \right] \quad (6)$$

where the constants C_i are determined from the following system of linear algebraic equations

$$\sum_{i=1}^N C_i P \left(\frac{a_k}{\lambda}; \frac{b_i}{\lambda} \right) + \frac{1 + a_k \lambda^{-1}}{a_k^2 \lambda^{-2}} L_N(0) + \sum_{j=1}^{\infty} G_j L_N(\lambda \mu_j) D \left(\frac{a_k}{\lambda}; \mu_j \right) = 0, \quad k = 1, 2, \dots, N \quad (7)$$

$$P(A; B) = \frac{B \text{ch } B + A \text{sh } B}{A^2 - B^2}; \quad D(A; \mu) = \frac{\mu \cos \mu + A \sin \mu}{A^2 + \mu^2 \lambda^2}$$

The distribution of the normal stresses on the crack plane in the radial direction is given by the following expression

$$p(r) = 2\pi^{-1} p \left\{ \arcsin \left(\frac{1}{r} \right) - \left[L(0) \Theta_0^{-1} + \sum_{n=1}^N C_n \text{sh}(\tilde{b}_n) + \sum_{j=1}^M G_j L_N(\lambda \mu_j) \right] \frac{1}{\sqrt{r^2 - 1}} - \sum_{k=1}^N L_N^k(\tilde{a}_k) \left[L(0) \Theta_0^{-1} + \sum_{n=1}^N C_n \frac{\tilde{a}_k^2 \text{sh}(\tilde{b}_n)}{\tilde{a}_k^2 - \tilde{b}_k^2} \right] \int_1^r \frac{\exp(-\tilde{a}_k(t-1))}{\sqrt{r^2 - t^2}} dt \right\}, \quad r > 1 \quad (8)$$

For the determination of the mode I stress intensity factor K_I one obtains

$$K_I = \lim_{r \rightarrow 1+0} \sqrt{r-1} p(r) = -\frac{\sqrt{2}}{\pi} p \Theta_0^{-1} \left(L(0) + \Theta(0) \left(\sum_{i=1}^N C_i \operatorname{sh} \tilde{b}_i + \sum_{j=1}^M G_j L_N(\lambda \mu_j) \right) \right) \quad (9)$$

Results.

Fig. 3 shows the changes in the mode I stress intensity factor when the crack radius varies in the range from $0.25H$ to $4.0H$ for the six different variation laws of the Young modulus in the vicinity of the crack for the oscillated load depicted in Fig. 2. The stress intensity factor is presented in a normalised form and calculated in accordance with Eq. 9. The numbered lines correspond to the heterogeneity law numbers as depicted in Fig. 1.

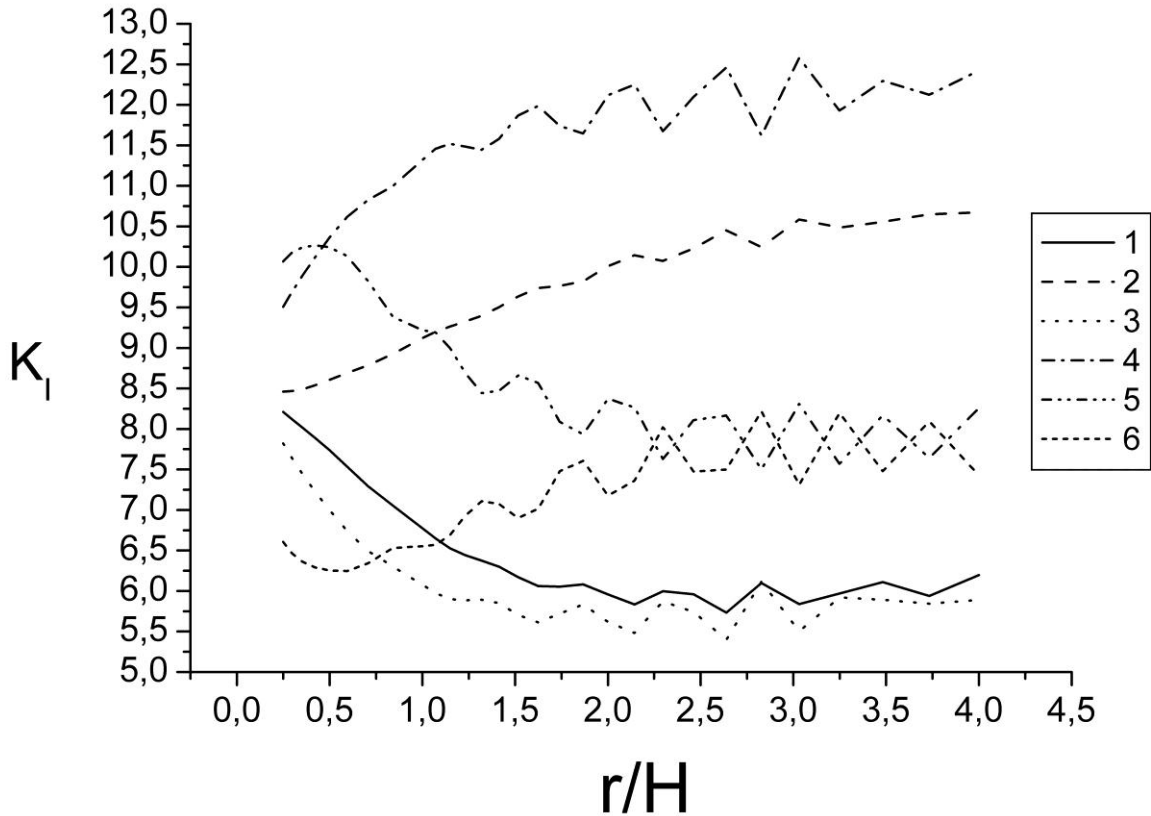


Fig. 3. Dependences of the dimensionless mode I stress intensity factor calculated by Eq. 9 vs crack radius for different heterogeneity laws (1-6 as depicted in Fig. 1)

For the sake of comparison Fig. 4 shows the dependences of the mode I stress intensity factors in the absence of the residual stresses for the same heterogeneous laws for variations of the Young modulus (the line marking is the same as in Fig. 3, apart from zero-marked line that represent the solution for the homogeneous space).

As it is evident from the results presented in Fig. 3-4, the mode I stress intensity factor is less affected by the residual stresses for the case of soft layers than in the other cases.

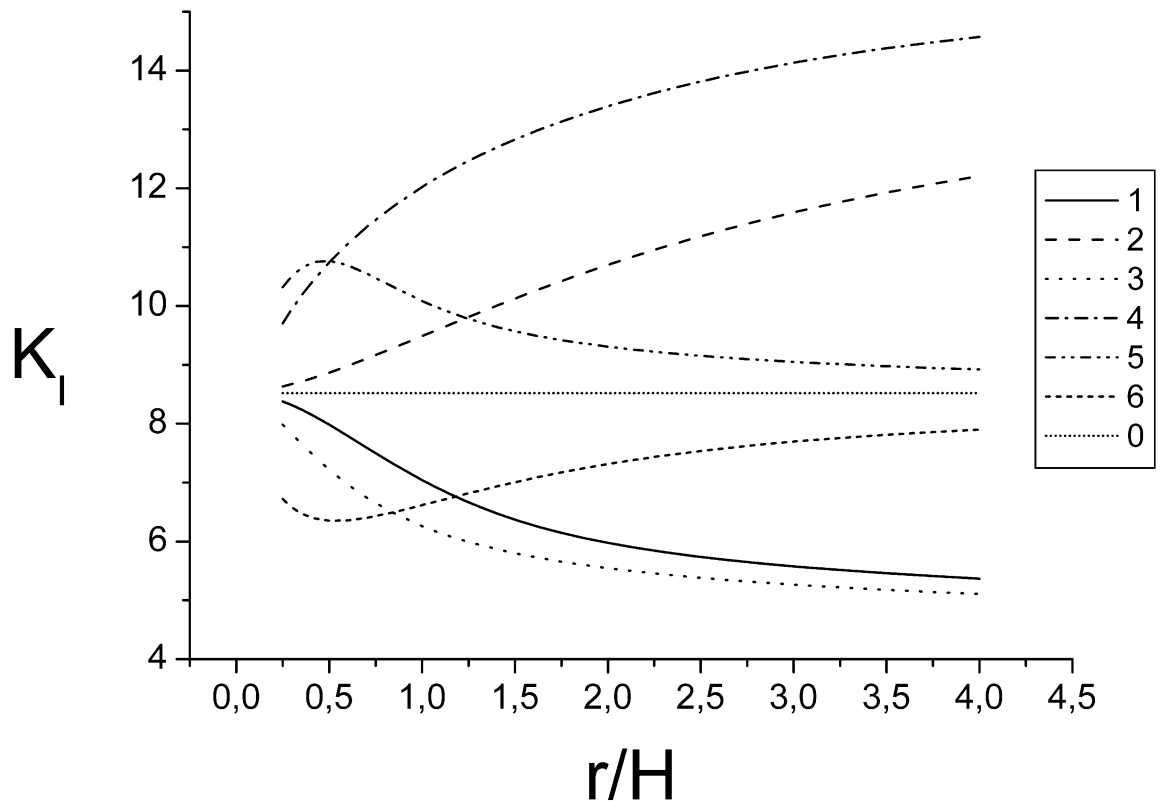


Fig. 4. Dependences of the dimensionless stress intensity factor calculated by Eq. 9 vs crack radius for different heterogeneity laws in the absence of residual stresses (same marking of heterogeneous laws as in Fig. 3 except for the straight line 0 that presents the constant dimensionless stress intensity factor in the homogeneous space)

Some cases when both the Young modulus and Poisson's ratio may vary with depth have also been analysed. Nine simple cases have been considered they assume that the moduli in the vicinity of a penny-shaped crack either uniformly increase or uniformly decrease with the depth as shown in Fig. 5. The loads acting on the crack surfaces are the same as those presented in Fig. 2, i.e. they combine an external load p_0 of unit intensity and the residual stresses, which intensity is of order between 10-20% of p_0 .

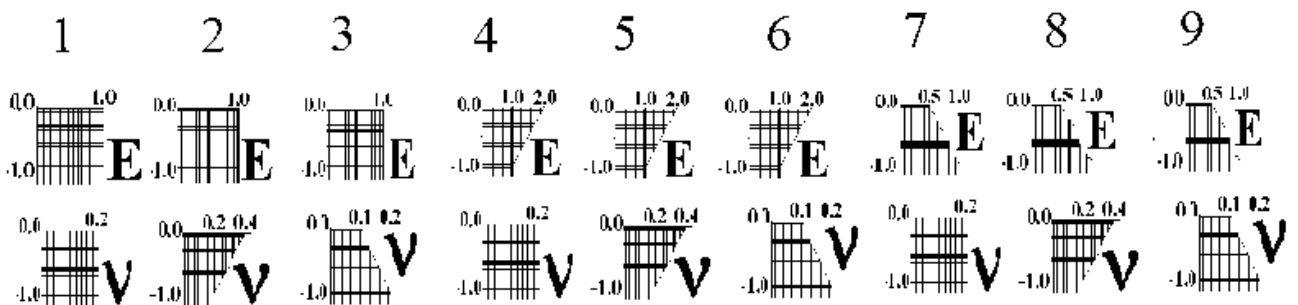


Fig. 5. Nine different combinations of the variations of elastic moduli in the vicinity of the crack

The analysis of the results of calculations of the mode I stress intensity factors for 9 different cases has shown that the variations in Poisson's ratio has little effect on the change of K_I in the presence of

residual stresses in the vicinity of the crack. On the other hand the variations of the Young modulus in the direction orthogonal to the crack surfaces affect the magnitude of K_I significantly in the presence of residual stresses.

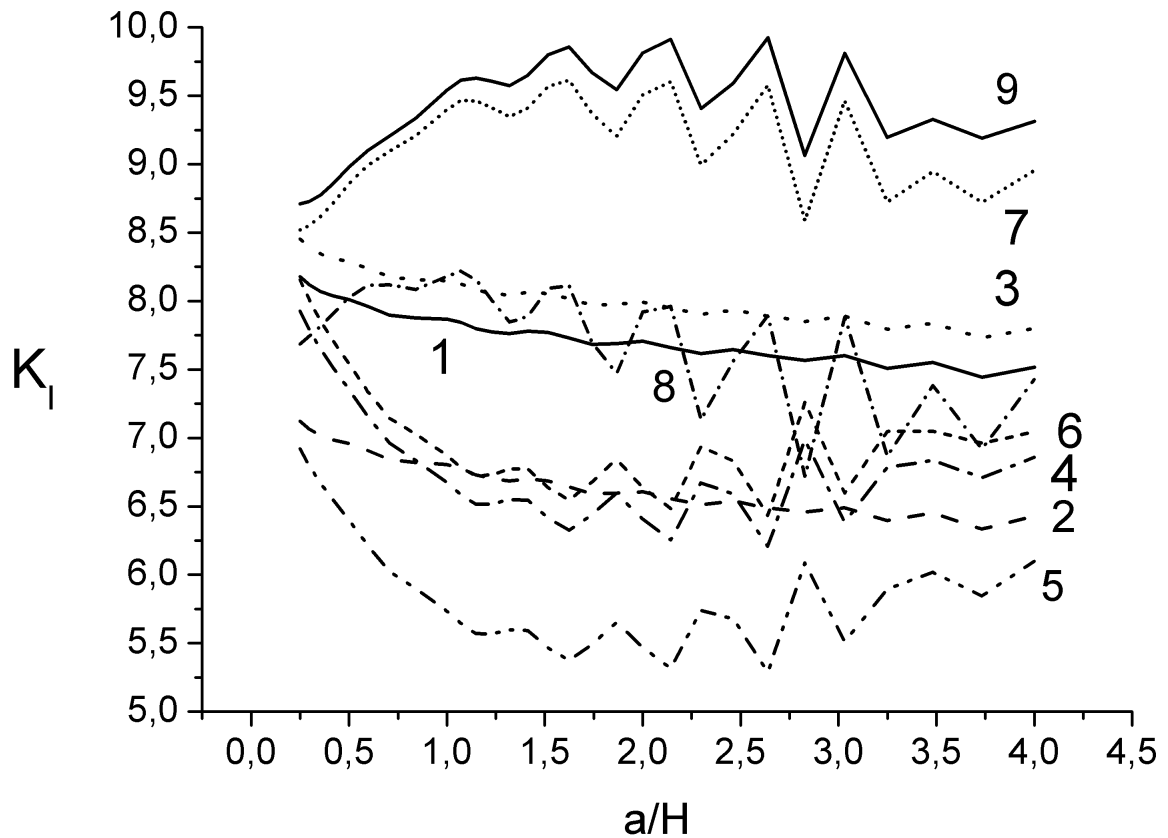


Fig. 6. Dependences of the dimensionless mode I stress intensity factors vs crack radius for different heterogeneity cases of variations of elastic moduli (the curves marked by numbers 1-9 correspond to the elastic moduli variation marked by the same numbers in Fig. 5) in

Conclusions.

We have developed a numerical approach capable of the determination of the mode I stress intensity factor for the penny-shaped crack that quasi-statically grows in a FGM subjected to the external loads and residual stresses. The method utilises the previously developed analytical approach for the consideration of axisymmetric problems reported in [1] and the approach suggested in [2] for taking into account the influence of residual stresses of random nature.

In the numerical experiments we have examined the case of co-sinusoidal distributions of the residual stresses and certain types of variation of the Young modulus as depicted in the Fig. 1 and the variations of both elastic moduli as shown in Fig. 5. The analysed typical distributions of the residual stresses along the crack radius are shown in Fig. 2, it is assumed that the intensity of the residual stresses is of order of 10-20% of the external load.

It has been shown that Poisson's ratio variations with the depth do not significantly affect the values of K_I . The influence of the residual stress fluctuations and the variations of the Young modulus on the mode I stress intensity factor is of the same order and much more pronounced than Poisson's ratio.

Acknowledgement. The authors are grateful for financial support provided by RFBR (grant №11-08-91168-ГФЕН_a, 12-07-00639_a), GK №11.519.11.3015, 11.519.11.3028, P1107

References

- [1] S.M. Aizikovich, V.M. Alexandrov, I.S. Trubchik and L.I. Krenev: Doklady Physics. Mechanics Vol. 54 (2009), p. 32
- [2] A.N. Galybin and A.V. Dyskin: International Journal of Fracture Vol. 128 (2004), pp. 95–103.
- [3] S.M. Aizikovich, V.M. Alexandrov and I.S. Trubchik, in: Modern Analysis and Applications, edited by Adamyan, V. M et al, volume 191 of Operator Theory: Advances and Applications, Birkhäuser Basel (2009).